Challenging Glass Conference Proceedings – Volume 8 – 2022 – Belis, Bos & Louter (Eds.)
Challenging Glass Conference 8 – 23 & 24 June 2022 – Ghent University – Ghent – Belgium
Conference on Architectural and Structural Applications of Glass

Experimental Investigation of a Transparent Interface Material for Glass Compression Members

Joseph Robert Yost [a], Matthew Cregan [b], Mohammad Bolhassani [c], Masoud Akbarzadeh [d], Yao Lu [d], Philipp Amir Chhadeh [e], Jens Schneider [e]

a Villanova University, USA, joseph.yost@villanova.edu
b Villanova University, USA
c City College of New York, USA
d University of Pennsylvania, USA
e Technische Universität Darmstadt, Germany

Abstract

In this experimental research a transparent thermoplastic manufactured by the DOW Corporation and known as Surlyn is investigated for use as an interface material in fabrication of an all-glass pedestrian bridge. The bridge is modular in construction and fabricated from a series of interlocking hollow glass units (HGU) that are geometrically arranged to form a compression dominant structural system. Surlyn is used as a friction-based interface between neighbouring HGUs preventing direct glass-to-glass contact. An experimental program consisting of axial loading of short glass columns (SGC) sandwiched between Surlyn sheets is used to quantify the bearing capacity at which glass fracture occurs at the glass-Surlyn interface location. Applied load cases include 100,000 cycles of cyclic load followed by 12 hours of sustained load followed by monotonic load to cracking, and monotonic loading to cracking with no previous load history. Test results show that Surlyn functions as an effective interface material with glass fracture occurring at bearing stress levels in excess of the column-action capacity of an individual HGU. Furthermore, load cycling and creep loading had no effect on the glass fracture capacity. However, the load history had a nominal effect on Surlyn, increasing stiffness and reducing deformation.

Keywords

Glass interface fracture, Transparent interface material, Bearing stress

Article Information

- Digital Object Identifier (DOI): 10.47982/cgc.8.395
- This article is part of the Challenging Glass Conference Proceedings, Volume 8, 2022, Belis, Bos & Louter (Eds.)
- Published by Challenging Glass, on behalf of the author(s), at Stichting OpenAccess Platforms

1. Introduction

As a civil engineering material, glass is most often used in commercial and residential construction as a transparent barrier between the interior and exterior environments. This is most often in the form of a non-structural façade attached to the exterior framing of the structure. In this application, glass functions as a plate resisting its own self-weight, which has an in-plane stressing effect, and wind loading, which acts transversely causing bending and shear. However, with recent advancements in glass manufacturing, structural detailing, and methods of analysis and design, glass is increasingly being used in a primary structural load bearing function. This is logical given the unique combination of transparency and high strength in compression. It is clearly understood, that with exploitation of these favourable characteristics, strict attention must be paid to the less favourable property of low tensile strength, tendency to crack and fracture. Considered collectively, a logical use of glass in a primary structural function suggests that of an axially loaded compression member resisting in-plane force. This is the intended function in construction of an all-glass pedestrian bridge with a geometric form that results in a compression dominant force resisting system (Akbarzahdeh et al. 2019). The geometric form of the bridge is found using three-dimensional graphic statics (3DGS) and form finding as described in Akbarzahdeh et al. (2015). A schematic of the proposed bridge is shown in Figure 1, where it is noted that a modular construction technique is proposed, with the bridge assembled as a collection of interconnected hollow glass units (HGU). An individual HGU is composed of two deck plates (top and bottom) and a collection of side plates (Figure 2), with connection between all plates made using a transparent double sided structural tape. Fabrication details of an individual HGU can be found in Lu et al. (2021) and Yost et al. (2021a). Importantly, all glass is cut to size using a robotically controlled five-axis abrasive water-jet.

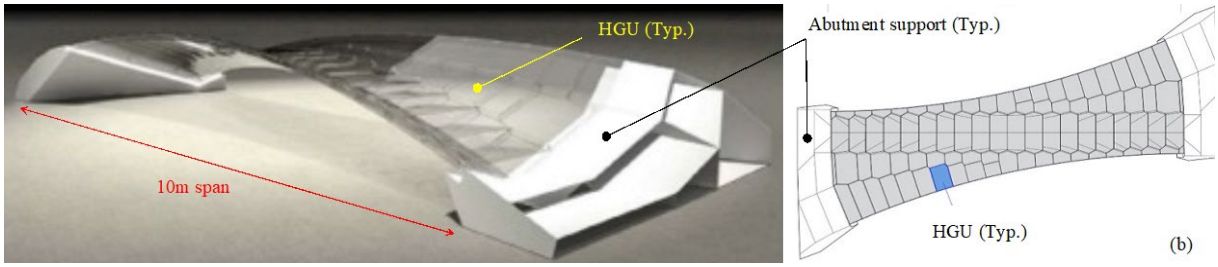

Fig. 1: Proposed all-glass pedestrian bridge. a) Isoparametric view, b) Plan view (taken from Yost et al 2021b)

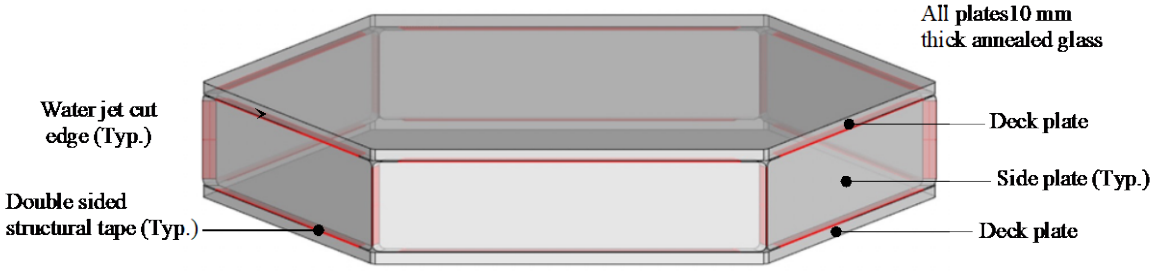

Fig. 2: Typical hollow glass unit (HGU).

In structural function, the HGU deck plates act in compression distributing dead and live load to the abutment supports. It is proposed that the HGUs be fabricated from 10 mm thick annealed glass. Feasibility of proposed modular glass system has been successfully demonstrated in experimental and numerical study of individual HGU strength and stiffness (Yost et al. 2021a). However, central to the

efficient collective function of HGUs assembled in a compression dominant form is in-plane force transfer between neighboring HGU deck plates. Clearly, there cannot be glass-to-glass contact and an interface material (IM) is required at the joint between neighboring HGU deck plates. Importantly, the IM must be transparent and have the necessary properties of stiffness and hardness to prevent fracture of the deck plate glass at the bearing surface. Of course, the deck plate glass fracture strength in bearing at the glass-IM zone is finite, and a minimum capacity is required so that the flexural buckling strength of the HGU deck plates in compression can be achieved. This minimum bearing strength is known from Yost et al. (2021a), where individual HGUs were tested in axial compression and a failure limit state by flexural buckling of the deck plates was achieved before any local fracture at the bearing locations occurred. In the study, oriented strand board (OSB) was used as the IM at the load and support locations. The bearing stress at flexural buckling was found to range from 30.1 to 36.9 MPa. Conservatively, a target bearing fracture capacity of 36.9 MPa is selected for the IM used in construction of the all-glass pedestrian bridge.

The need for an interface material to facilitate force transfer with glass is fundamental to the materials structural function. For example, previous experimental research has implemented an “interface material” applied as a dry connection to separate glass test samples in compression from the steel surfaces of a testing machine. Materials such as thermoplastic layer (Aiello at al. 2011), PMMA pad (Zhao et al. 2020), aluminum, lead (Oikonomopoulou et al. 2017), or simply wood (Veer et al. 2020) are all used to prevent premature cracking during experimental testing. Actual applications of a soft transition material outside of a lab setting can be found through projects led by Delft University of Technology (Netherlands). This institution has developed a design for an all-glass structure made from cast glass blocks, where polyurethane rubber is used as an interface between neighboring glass blocks (Oikonomopoulou et al. 2018a). The construction of the Crystal House in Amsterdam, Netherlands, utilized an adhesive bonding material between individual glass bricks to create an all-glass façade. The base of this glass wall rested on stainless steel plates to separate it from the concrete foundation (Oikonomopoulou et al. 2018b). In larger structural applications, structural silicone is used to bond the glass at joints (de Krom et al. 2020a 2020b).

2. Preliminary Material Selection

A preliminary experimental investigation, designated Phase I, was executed where multiple candidate transparent interface materials were considered. These included acrylic, polyvinylchloride (PVC), polycarbonate, and Surlyn. Surlyn is a transparent thermoplastic material manufactured by the Dow Corporation. Surlyn is often used for orthotics and prosthetics, and is characterized by high toughness, strong durability, and good resistance to chemical attack (Surlyn 2022). Surlyn is available in flat sheets between 3 and 12 mm thick.

Short glass columns were assembled from 10 mm thick annealed glass, and tested in axial compression with the IM located between the glass bearing surfaces and the load and support apparatus of the servo-controlled MTS hydraulic test machine. The bearing surface of the glass was cut using an abrasive water-jet, the same as will be used in fabrication of the proposed pedestrian bridge. A typical detail of the Phase 1 short column test setup is shown in Figure 3. Cracking strength results from this preliminary phase of testing are shown in Table 1. The bearing capacity of acrylic ranged from 8.58 to 15.5 MPa, well below the target value of 36.9 MPa. The same is true for polycarbonate, with a strength range between 30.2 and 32.5 MPa, again below the target value. The results for PVC were also not favorable, where a strength range of between 16.0 to 26.8 MPa, and as with acrylic, well below the target value

of 36.9 MPa. Surlyn, however, performed as required with cracking strength ranging from 39.1 MPa to 42.5 MPa, all in excess of the minimum target of 36.9 MPa.

From the results of Table 1, acrylic, polycarbonate, and PVC were eliminated as potential interface material, and it was decided to select Surlyn as the interface material for further detailed study.

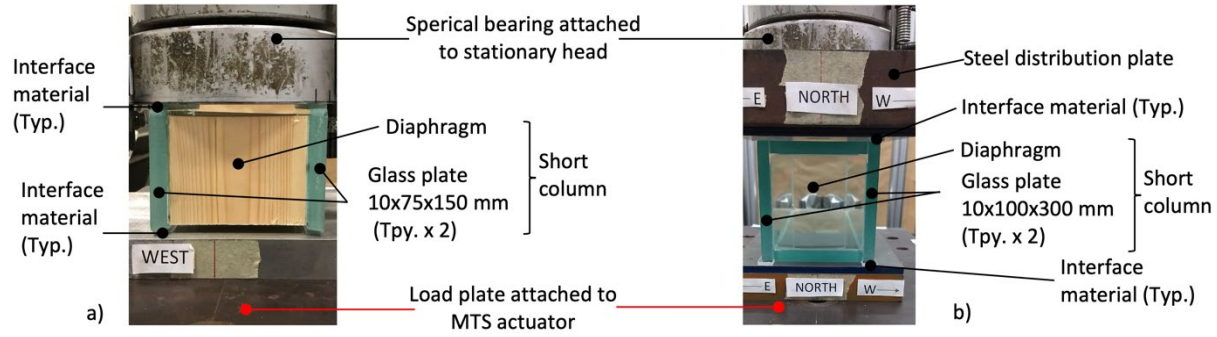

Fig. 3: Phase I - Preliminary test setup. a) Samples 1-to-4, b) Samples a-to-f

Table 1: Preliminary test results.

Specimen	Interface Material	Cracking strength (MPa)	Strength / Target (-)
1, 2	Acrylic	8.58, 15.5	0.23, 0.42
3, 4	Polycarbonate	32.5, 30.2	0.88, 0.82
a, b, c	PVC	26.8, 16.0, 21.4	0.73, 0.43, 0.58
d, e, f	Surlyn	40.2, 39.1, 42.5	1.09, 1.06, 1.15

3. Experimental Program

The objective of the experimental program was to measure the cracking potential of annealed glass having an abrasive water-jet cut edge and in bearing against Surlyn. To achieve this objective, test samples were designed as short columns of very low slenderness and loaded in axial compression with Surlyn as the interface material between the glass and loading apparatus. A typical sample detail is shown in Figure 4, where it is noted that the sample consists of two column plates (E and W sides) and two diaphragm plates (N and S sides). All glass plates were 10 mm thick annealed float-glass, had a 5 mm radius corner fillet, and were cut to size using an abrasive water-jet. Column and diaphragm plates had dimensions width x height of 102 x 102 mm and 95 x 80 mm, respectively. The connection between column and diaphragm plates was made using a transparent double-sided structural tape known as Very High Bond tape (VHB). An exploded view of this connection is shown in Fig. 4c, where the abrasive water-jet surface texture of the column plate is noted. VHB is manufactured by the 3M company (3M VHB 2021) and had dimensions of 1 mm thick and was trimmed to a width of 10 mm to match the glass thickness. The Surlyn interface was placed top and bottom as a continuous sheet spanning between column plates. The Surlyn was intentionally sized this way so that the loaded outside edge was a free surface and the loaded inside edge was a continuum of interface material.

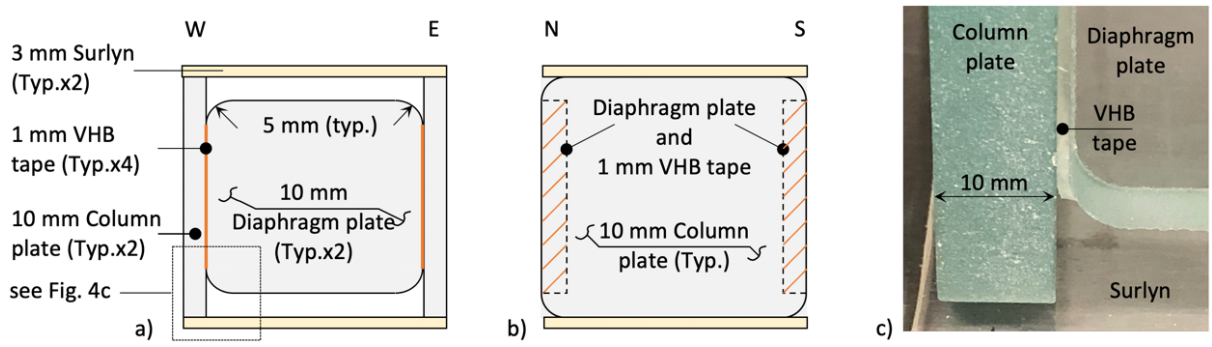

Fig. 4: Sample details. a) E-W view, b) N-S view, c) Exploded view of connection

All samples were tested in a MTS servo-hydraulic test machine with a steel loading frame attached to the actuator on bottom, and a spherical bearing attached to a stationary support at top. Test were run under ambient indoor temperature and humidity. Vertical displacement was measured between the inside surfaces of the load and support apparatus at all four corners (NE, NW, SE, and SW) using potentiometers with 15 mm travel. All force and displacement and data was acquired by a 16-bit data acquisition system.

The load protocol included three phases, which are stress cycling (designated CY), sustained stress or creep (designated CR), and finally monotonic loading to failure (designated MF). Stress cycling (CY) included 100,000 cycles at a stress range of between 5 and 15 MPa, and at a rate of 1 Hz. This stress range corresponds to that expected from dead load (D) and dead load plus live load (D+L) in the proposed pedestrian bridge. During this phase 2 cycles of data were captured every 50 cycles at a data recording rate of 100 Hz. Load cycling was followed by a creep phase (CR), where stress was held constant at 5 MPa (corresponding to DL) for 12 hours, and data was acquired continuously at a rate of 1 Hz. Next, the sample was unloaded and immediately tested monotonically to failure in displacement control at a rate of .1 mm/minute and with data acquired at a rate of 10Hz. To measure any effect of load cycling and creep loading on the glass cracking potential and behavior of the Surlyn interface material, a control set of samples were tested monotonically to failure with no previous history of load cycling or creep.

In total, six samples were tested, three samples subjected to all three load phases (CY, CR and MF in that order), designated CY-CR-MF-a,b,c, and three samples loaded to failure with no previous load history, designated 00-00-MF-a,b,c.

4. Test Results

Presentation of test results is made with regard to the load history. With this as context, presented first are the results from the cyclic and creep loading phases of the test program, which includes the CY-CR-00-a,b,c test results for three samples. This data characterizes Surlyn's force-deformation response to the imposed cyclic and creep loading and how this response changes with cycle number and time. In effect, from the imposed stress levels this represents the service limit state response of Surlyn as an interface material. This is followed by the monotonic test to failure results, where samples are loaded monotonically in displacement control until slightly beyond glass fracture and unloaded. These results include 6 samples total, six tests for cy-cr-MF-a,b,c, samples that have experienced cyclic and creep loading, and three tests for 00-00-MF-a,b,c, samples with no previous load history. The monotonic failure results are significant in first characterization of Surlyn's behavior as a function of

force (or stress) and second the fracture potential of float glass with Surlyn as the interface material. The latter is a measure of Surlyn's feasibility as an interface material able to resist glass fracture so that limit states related to column behavior are achievable, which is central to the material's effective function.

Displacement results represent the average of the four potentiometers located in the four corners of the short column sample and positioned between the inside surfaces of the top and bottom load apparatuses. Thus, displacement represents the compression deformation in the Surlyn layers (top and bottom).

4.1. Cyclic and Creep Results

The results for cyclic and creep loading include three samples, CY-CR-00-a, CY-CR-00-b, CY-CR-00-c, and are presented in Figure 5 as displacement verses time, where displacement is plotted at both □max and □min for the cyclic phase (CY) of the test. Again, displacement represents the average of the four potentiometers and is a measure of Surlyn's compression deformation. The results show all samples follow a very similar behavior, with accelerated displacement growth in about the first 10,000 cycles, followed by a flattening with continued displacement growth to 100,000 cycles, albeit at a much-reduced rate. The initial displacement at □max varies from a high for CY-CD-00-b of 0.285 mm to a low for CY-CD-00-c of 0.224 mm, however the difference between displacements at □max and □min is about the same for all samples, and equal to about 0.60 mm. This suggests that the deflection change as a function of number of load cycles is approximately the same at both maximum and minimum load. These cyclic phase results are favorable for Surlyn as an interface material subjected to load cycling, as would be the case in a pedestrian bridge application. It is noted that at the end of cyclic loading the change in deflection for samples CY-CR-00-b and CY-CR-00-c is essentially zero, and for sample CY-CR-a, the rate is increasing at about the same rate as since 80,000 cycles.

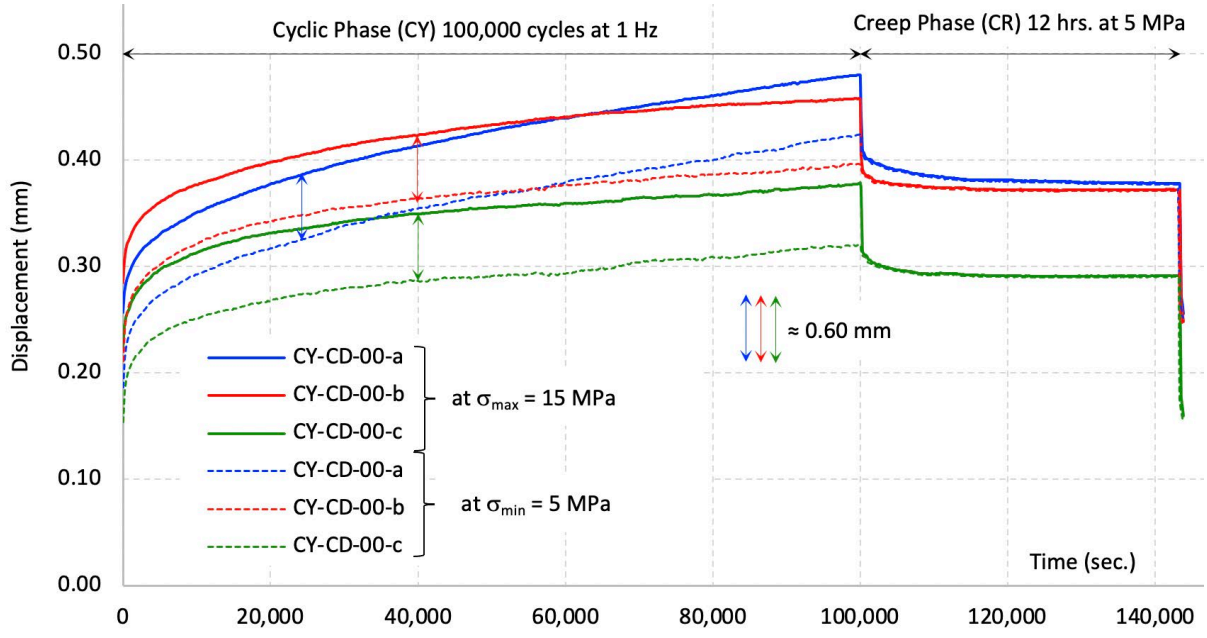

Fig. 5: Test results for cyclic and creep loading phases.

During the creep loading phase (CR) the displacement at the start is .406, .388 and .311 mm for samples CY-CD-00-a, CY-CD-00-b, and CY-CD-00-c, respectively. After 12 hours of sustained load at 5 MPa, the end of the creep phase, these displacements are .377, .372 and .291 mm, respectively. This translates to a change of -7.1, -4.1 and -6.8%, respectively. As is noted from Figure 5, the majority of this recovery takes place in the first 5,000 second of the CR phase, after which the displacement is essentially flat. These creep results for Surlyn are favorable and suggest stable dimensional measure under sustained load.

4.2. Monotonic Failure Results

After the creep loading phase of Samples CY-CR-00-a,b,c, load was completely removed, the data acquisition was zeroed, and these samples were monotonically loaded to failure. These test results are designated cy-cr-MF-a,b,c. As well a set of three control samples with no previous load history were monotonically tested to failure, and designated 00-00-MF-a,b,c. The monotonic test to failure results for these six samples are shown in Figure 6, and the cracking strength results are summarized in Table 2. In the test procedure, all samples were unloaded shortly after the first crack occurred, and the glass was not crushed.

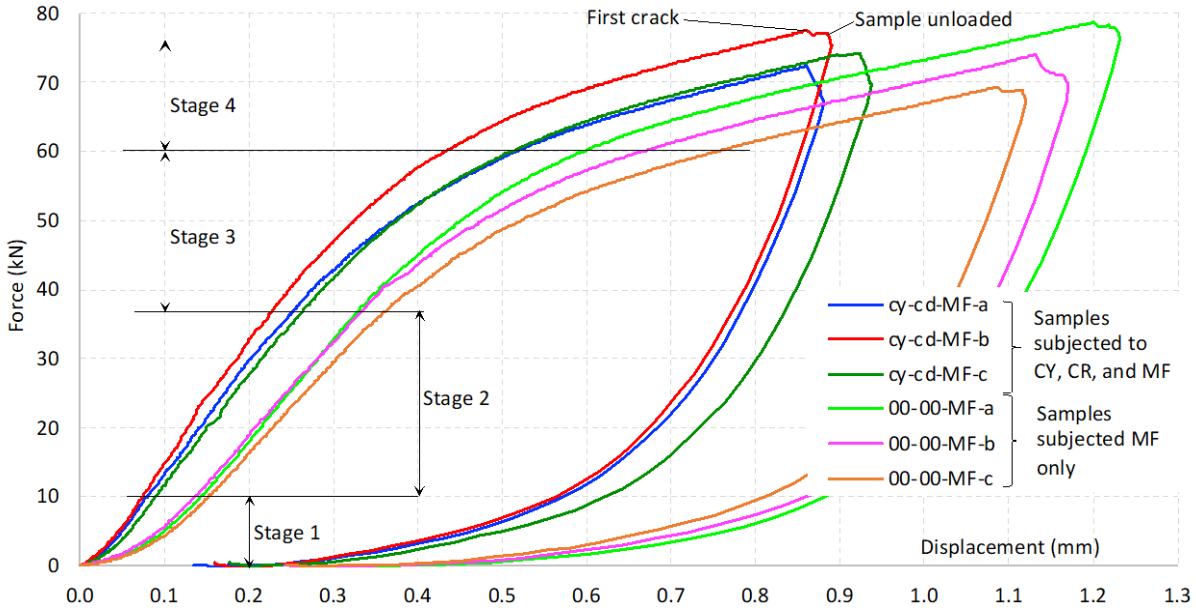

Fig. 6: Test results for monotonic failure phase.

Table 2: Summary of test results.

Sample	Force at first crack (MPa)	Stress at first crack (MPa)	Cracking strength / Target (-)
CY-CD-MF-a	72.5	41.6	1.13
CY-CD-MF-b	77.8	44.6	1.21
CY-CD-MF-c	74.2	42.5	1.15
00-00-MF-a	78.7	45.1	1.22
00-00-MF-b	74.1	42.5	1.15
00-00-MF-c	69.5	39.8	1.08

The results of Figure 6 show that cyclic and creep loading do have an effect on the force-displacement response at low level loading. As can be seen, application the cyclic and creep loading result in a stiffer response for loads below about 10 kN. In fact, the average displacement at 10 kN for the three samples experiencing cyclic and creep loading is .0813 mm, and for samples with no prior load history, this average is 0.144 mm, or 77% higher. In general, the force-displacement response for both sample groups (cy-cr-MF and 00-00-MF) is similar, with nonlinear initial response (Stage 1 in Fig. 6), followed by an approximately linear response (Stage 2 in Fig. 6), followed by a nonlinear transition region (Stage 3 in Fig. 6), and ending with approximately linear behavior to cracking (Stage 4 in Fig. 6). It is also clear from Fig. 6 that the displacement at cracking is significantly lower for the samples experiencing cyclic and creep loading. Specifically, the average displacement at cracking for sample groups cy-cd-MF and 00-00-MF is 0.871 and 1.14 mm, respectively. Thus, applying load cycling and creep results in a measurable increase in stiffness and decrease in displacement at cracking of about 24%.

The first crack in all cases had a characteristic appearance, described as a “shell” shape, as is shown in Fig. 7. The crack always formed within the 10 mm glass thickness and propagated along the length of the bearing area, and through the column plate height. A print of the crack could be easily seen on the Surlyn surface in bearing with the glass (Fig. 7). The orientation of this crack suggests potentially that contact tension stress exists across the glass thickness in bearing with the Surlyn ultimately triggering crack propagation.

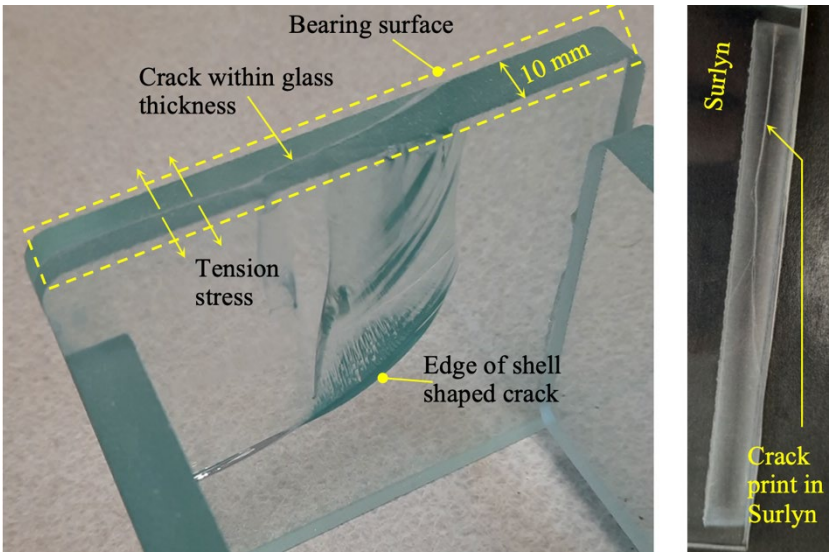

Fig. 7: Typical crack pattern.

The results of Table 2 provide the magnitude of force and corresponding bearing stress at the appearance of first crack, and the last column gives the ratio of this bearing stress to the target bearing stress of 36.9 MPa. The results are very encouraging, and all six samples exceeded the target value. Overall, the range of Cracking strength / Target strength was between 1.08 and 1.21, with an overall average of 1.16. Comparing groups CY-CD-MF and 00-00-MF, the three-sample average is 1.13 and 1.15, respectively. This is important and signifies that the cyclic and creep loading had essentially no effect on the cracking strength of the glass. This result is specific to the load cycling and sustained load applied in this study, but the result is promising for using Surlyn where cyclic and sustained load is expected.

5. Conclusions

In this research study Surlyn was experimentally evaluated as a transparent interface material in bearing against 10 mm thick annealed glass. The glass had a surface texture corresponding to that from cutting using an abrasive water-jet. Two load cases were considered; a) cyclic load followed by creep load followed by monotonic test to failure, and b) monotonic loading to failure with no previous load history. A target bearing stress was selected of 36.9 MPa, which corresponds the bearing stress necessary to achieve a flexural buckling failure limit state in glass plates with in-plane axial load. The following conclusions are found:

- Cyclic and creep loading had no effect on the cracking strength of the glass. The average ratio of cracking strength to target strength for samples experiencing cyclic and creep load was 1.15, and this ratio was 1.13 for samples with no prior load history. By this measure, cyclic and creep loading do not affect the bearing stress at which glass in contact with Surlyn will crack.
- The crack shape was that of a shell, forming through the 10 mm glass thickness and propagating along the bearing length. The crack orientation suggests the presence of contact tension stress perpendicular to the long bearing direction.
- In general, all samples had a force-displacement characterized by an initial nonlinear response, followed by a linear region in the service load range, after which there was a nonlinear transition to a less stiff linear region ultimately ending in cracking.
- Cyclic load and sustained load did have a measurable effect on the stiffness of the initial nonlinear region and following linear service load region.
- Displacement at cracking was, on average, 24% less for samples experiencing cyclic and creep loading as compared to samples with no prior load history.

Acknowledgements

This research was supported by University of Pennsylvania Research Foundation Grant (URF), United States, National Science Foundation CAREER AWARD, United States (NSF CAREER-1944691- CMMI) and the National Science Foundation Future Eco Manufacturing Research Grant, United States (NSF, FMRG-CMMI 2037097) to Dr. Masoud Akbarzadeh. Also, this study was supported by Villanova University Summer Grant Program (USG), and Villanova University Department of Civil and Environmental Engineering Graduate Student Support Program (GSSP), United States, to Dr. Joseph Robert Yost.

References

Aiello S, Campione G, Minafo G, Scibilia N: Compressive behaviour of laminated structural glass members. Engineering Structures 33 (2011). pp. 3402-3408. https://doi.org/10.1016/j.engstruct.2011.07.004

Akbarzadeh M, Van Mele T, Block P: On the equilibrium of funicular polyhedral frames and convex polyhedral force diagrams. Comput Aided Des (2015); 63:118–28.

Akbarzadeh M, Bolhassani M, Nejur A, Yost J R, Byrnes C, Schneider J: The design of an ultra-transparent funicular glass structure. Proceedings ASCE Structures Congress. Orlando, Florida (2019); URL https://ascelibrary.org/doi/pdf/10.1061/9780784482247.037

de Krom D, ten Brincke E, Hagen C, Ramadas S B, Hoogendoorn W: 100% Transparent Floating Glass Boxes. Challenging Glass 7 (2020a); Ghent University. https://doi.org/10.7480/cgc.7.4546

de Krom D, Veer F, Riemens K, Hoogendoorn W: Façade becomes structure. Challenging Glass 7 (2020b); Ghent University. https://doi.org/10.7480/cgc.7.4545

Lu Y, Cregan M, Chhadeh P A, Seyedahmadian A, Bolhassain M, Schneider J, Yost J R, Akbarzadeh M: All glass, compression-dominant polyhedral bridge prototype: form-finding and fabrication. Proceedings of the IASS Annual Symposium. Guilford, UK (2021); URL https://www.researchgate.net/publication/355379350_All_glass_compression-dominant_polyhedral_bridge_prototype_form-finding_and_fabrication

Oikonomopoulou F, Bristogianni T, Barou L, Jacobs E, Frigo G, Veer F A, Nijsse R: A novel, demountable structural glass system out of dry-assembly, interlocking cast glass components. Challenging Glass 6 (2018a); Milan, Italy. https://doi.org/10.7480/cgc.6.2118

Oikonomopoulou F, Bristogianni T, Veer F, Nijsse R: The construction of the Crystal Houses façade: challenges and innovations. Glass Structures Engineering (2018b); vol 3 pp 87-108. https://doi.org/10.1007/s40940-017-0039-4

Oikonomopoulou F, van den Broek E A M, Bristogianni T, Veer F, Nijsse R: Design and experimental testing of the bundled glass column. Glass Structures Engineering (2017); pp. 183-200. https://doi.org/10.1007/s40940-017-0041-x

Surlyn (2022) URL https://www.curbellplastics.com/Research-Solutions/Materials/Surlyn

Veer F, Nijsse R, Baardolf K, Vitalis D, Lenk P: The Development and Testing of Large Sandwich Panels. Challenging Glass 7 (2020); Ghent University. https://doi.org/10.7480/cgc.7.4488

Yost J R, Bolhassani M, Chhadeh P A, Ryan L, Schneider J, Akbarzadeh M: Mechanical performance of polyhedral hollow glass units under compression. Engineering Structures (2021a); URL https://doi.org/10.1016/j.engstruct.2021.113730.

Yost J R, Akbarzadeh M, Bolhassani M, Ryan L, Schneider J, Chhadeh P A: Behavior of Polyhedral Built-Up Glass Compression Members. J. of Architectural Design and Construction Technology (2021b); 2(3): 1-7. URL https://helicsgroup.net/assets/articles/1630327044.pdf.

Zhao S, Chen S: Experimental Investigation on the Structural Performance of Square Hollow Glass Columns Under Axial Compression. Challenging Glass 7 (2020); Ghent University. https://doi.org/10.7480/cgc.7.4473

3M VHB, structural glazing tape (2021) URL https://www.3m.com/3M/en_US/p/d/b40072022/

Challenging Glass Conference Proceedings – Volume 8 – 2022 – Belis, Bos & Louter (Eds.)
Challenging Glass Conference 8 – 23 & 24 June 2022 – Ghent University – Ghent – Belgium
Conference on Architectural and Structural Applications of Glass

Platinum Sponsors

SAINT-GOBAIN

EASTMAN

Gold Sponsors

Bellapart

DOW

kuraray

Trosifol®

SentryGlas®

sedak

SEEN

Silver Sponsors

octatube

PERMASTEELISA GROUP

vitroplena
structural glass solutions

Organising Partners

GHENT UNIVERSITY

TU/e

TU Delft